

Capture-Gamma Determination of V^{52} Levels*†

J. E. SCHWÄGER‡

Lawrence Radiation Laboratory, University of California, Livermore, California

(Received July 13, 1960; revised manuscript received October 7, 1960)

Thermal-neutron capture-gamma radiations for the $V^{51}(n,\gamma)V^{52*}$ reaction have been observed with a fast-coincidence scintillation spectrometer recently developed for the Livermore 1-Mw pool-type reactor. The added-neutron binding energy in V^{52} was measured as 7.30 ± 0.05 Mev and a decay scheme was established which verifies a previously proposed $V^{51}(d,p)V^{52*}$ level scheme. Several low-energy crossover, without stopover, transitions were observed: two from the 0.78-Mev level to the ground and 0.13 levels (the latter being the more intense) but not to the 0.42 level, and one from the 0.83-Mev level to the ground state only. The 0.42-Mev level makes both crossover and stopover transitions to the ground and 0.13-Mev levels (the former being the stronger). Some evidence exists to suggest that the low-lying V^{52*} states arise from excitations of the $(1f_{7/2})^3$ proton configuration alone.

INTRODUCTION

EXCITED states in V^{52*} have been determined principally by results from the $V^{51}(d,p)V^{52*}$ reaction and interpretation of gamma rays observed in $V^{51}(n,\gamma)V^{52*}$ experiments. Considerable disagreement existed in the early work,¹⁻⁴ the capture-gamma experiments showing a much more complicated spectrum than would be expected from the initial (d,p) studies. In order to clarify these earlier discrepancies, Schwäger and Cox⁵ studied the $V^{51}(d,p)V^{52*}$ reaction with higher resolution apparatus than had been available to other workers and observed 23 proton groups corresponding to V^{52*} levels up to 3.31-Mev excitation. This work was in good agreement with the $V^{51}(n,\gamma)V^{52*}$ high-energy capture-gamma studies performed by Bartholomew and Kinsey⁶ as well as the more recent extensive (n,γ) work by Groshev *et al.*⁷⁻⁹ Also El Bedewi and Tadros¹⁰ have currently completed a (d,p) study of V^{52*} which, with the exception of some complex levels that their lower resolution apparatus was not able to probe, is in good agreement with Schwäger and Cox.

* Work was performed under the auspices of the U. S. Atomic Energy Commission.

† These results are taken from a thesis submitted by the author to the University of California in partial fulfillment of the requirements for the degree of Doctor of Philosophy in Physics.

‡ Commander, U. S. Navy, on special assignment at the Lawrence Radiation Laboratory.

¹ W. L. Davidson, Phys. Rev. **56**, 1061 (1939).

² V. S. Abramov, Doklady Akad. Nauk S.S.S.R. **73**, 923 (1951).

³ J. A. Harvey, Phys. Rev. **81**, 353 (1951).

⁴ J. S. King and W. C. Parkinson, Phys. Rev. **89**, 1080 (1953).

⁵ J. E. Schwäger and L. A. Cox, Phys. Rev. **92**, 102 (1953).

⁶ G. A. Bartholomew and B. B. Kinsey, Phys. Rev. **89**, 386 (1953).

⁷ L. V. Groshev, B. P. Ad'yasevich, and A. M. Demidov, *Proceedings of the Conference of the Academy of Sciences of the U.S.S.R. on the peaceful Uses of Atomic Energy, Moscow, July 1955* (Akademiia Nauk S.S.S.R. Moscow, 1955) [English translation by Consultants Bureau, New York: U. S. Atomic Energy Commission Report TR-2435, 1956], Vol. 4, p. 270.

⁸ L. V. Groshev, B. P. Ad'yasevich, and A. M. Demidov, *Proceedings of the International Conference on the Peaceful Uses of Atomic Energy, Geneva, 1955* (United Nations, New York, 1956), Vol. 2, p. 39.

⁹ L. V. Groshev, A. M. Demidov, V. N. Lutsenko, and V. I. Pelekhov, *Atomnaya Energ.* **3**, 187 (1957).

¹⁰ F. A. El Bedewi and S. Tadros, *Nuclear Phys.* **8**, 71 (1958).

Most of the previous extensive investigations of gamma rays following thermal neutron capture have concentrated on obtaining the singles spectra of the emitted radiations under as high a resolution as possible. Although some features of a decay scheme are often inferred from the energies and intensities of the gamma rays present, usually it is impossible to deduce an unambiguous scheme even with excellent resolution because the spectra are so complex. Since there is particular interest in the lower excited states of nuclei for theoretical reasons, it is desirable to establish decay schemes to help determine level character. Furthermore, it is interesting to compare the low-excitation behavior of V^{51*} vs V^{52*} so as to observe the change in $(1f_{7/2})^3$ proton configuration coupling of V^{51*} introduced by the additional coupling of a $(2p_{3/2})$ neutron in V^{52*} . Unfortunately Bartholomew and Kinsey⁶ were restricted to observations of gammas > 3 Mev (pair spectrometer); but Groshev *et al.*,⁷⁻⁹ using a Compton-recoil beta spectrometer, are able to observe low-energy singles radiation. The latter instrument, however, magnetically analyzes Compton-recoil electrons emerging in the forward direction and consequently cannot be sensitive in the low-energy region because the differential cross section is small for such Compton electrons. Additionally, V^{52} is not stable and beta decays to Cr^{52} with the emission of 1.43 radiation¹¹ which makes conventional exploration of this energy region impossible. Consequently, it was

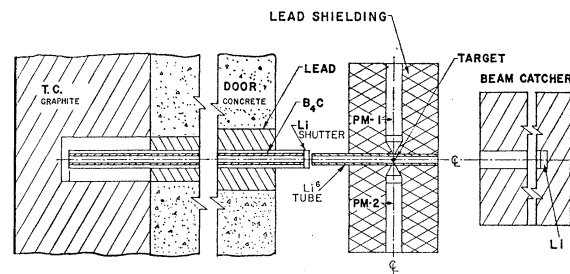
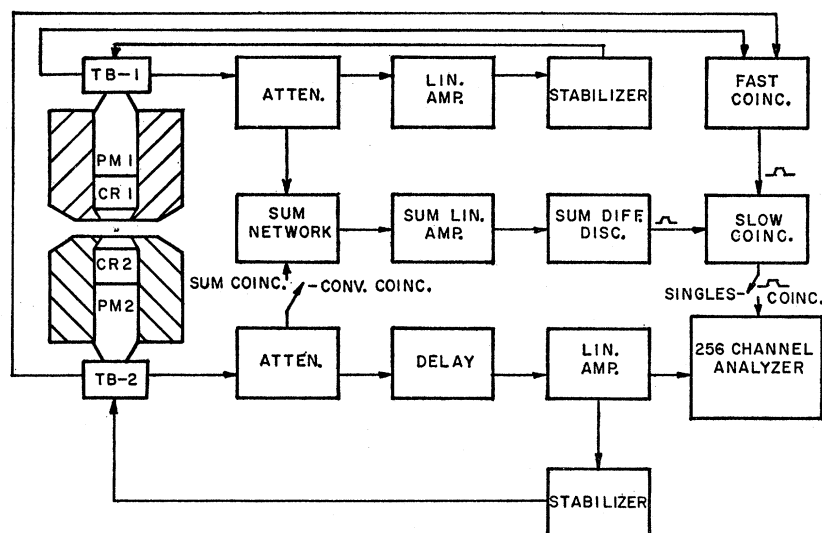


FIG. 1. Schematic of the experimental geometry.

¹¹ All energies in this paper are reported in Mev units.

FIG. 2. Block diagram of spectrometer.



thought desirable at Lawrence Radiation Laboratory (LRL) to explore the low-energy region of V^{52*} radiation with a gamma-gamma coincidence spectrometer to establish the decay scheme and to check those portions of the (d,p) level scheme that have not yet been confirmed.

EXPERIMENTAL TECHNIQUE

High-resolution beta-ray spectrometers and crystal diffraction spectrometers unfortunately have an inherent low yield which, with the neutron fluxes presently available, makes them impractical for gamma-gamma coincidence investigations. Thus, in spite of the relatively poor resolution obtained, a scintillation technique must be used for this application. Scintillation detectors, however, produce a complex response (Compton tails, escape peaks, bremsstrahlung smears) for incident monoenergetic radiation which makes it difficult to interpret complicated spectra. An especially promising solution for this problem is to employ the sum-coincidence technique recently proposed by Hoogenboom.¹²

Figure 1 (not to scale) is a schematic of the experimental geometry showing the target being irradiated by a narrow external thermal neutron beam which is piped from the thermal column of the Livermore 1-Mw pool-type reactor. For reactor operations at a given power level, the desired neutron beam intensity is obtained by a proper choice of cavity depth in the thermal column and/or by positioning the target. The neutron collimator section in the target assembly is a canister of Li^6 sealed between two thin-walled aluminum tubes. This provides a $\frac{3}{4}$ -in. diam neutron beam at the target and protects the NaI crystals from scattered neutrons. For coincidence work, the crystals can be placed to within $\frac{3}{4}$ in. of the target center line. A pair

of 2-in.-diam by 2-in.-long NaI(Tl) cylindrical crystals with RCA 6655-A photomultipliers are used.

Figure 2 is a block diagram of the spectrometer showing the fast-slow coincidence system with conventional and sum-coincidence options. A fast signal is taken from the anode of the photomultiplier and passed through a limiting stage in the tube base which is adjusted to limit all but the weaker pulses associated with less than 0.6-Mev gammas. For a facing crystal geometry, conical lead shields reduce but do not eliminate unwanted coincidences caused by secondary radiation produced in the shielding and by back-scattered or annihilation quanta from the opposing crystal. These unwanted spurious coincidences can be further controlled by setting the trigger level of the fast-coincidence unit to eliminate them when gammas of interest have energies greater than 0.51 Mev. The fast-coincidence unit is operated with resolving times between 3×10^{-8} and 5×10^{-8} sec, depending upon the trigger setting.

A slow signal is taken from the seventh dynode, delay-line-clipped to produce a well-formed 10^{-6} -sec wide pulse, and fed in parallel to a linear amplifier and an adding circuit (a simple resistor network). Proper operation of the adding network for the sum-coincidence mode depends upon identical (and completely linear) energy calibration of both photomultipliers. Linearity is assured by individually stabilizing the anode and the last five dynode voltages of the photomultiplier. Calibrations are matched through a coarse adjustment with the attenuator strip and a fine adjustment with the high voltage. Each photomultiplier spectrum is individually stabilized by applying correction voltages to the photomultiplier cathode from a counting-rate-difference feedback network of the de Waard type.¹³

The sum-coincidence method for capture-gamma

¹² A. M. Hoogenboom, Nuclear Instr. 3, 57 (1958).

¹³ H. de Waard, Nucleonics 13, No. 7, 36 (1955).

work is based upon the simple fact that in any nuclear decay scheme caused by gamma de-excitation from a thermal neutron capture state to the ground state, the energies of all gammas related in cascade must sum to the neutron binding energy. In particular, a two-crystal apparatus looks primarily at double cascades with sums equal to the neutron binding energy. As a consequence, the sum-coincidence spectrum shows only the full energy peaks of the double cascade gamma rays (the order in which the cascade occurs will be unknown, however) and removes most of the ambiguity faced in trying to determine distinct nuclear levels.

Unfortunately, the sum-coincidence method just outlined did not work well in practice at the LRL installation. One of the two radiations involved in a capture-gamma double cascade is always >4 Mev because the neutron binding energy is ≈ 8 Mev. Since pair production is the dominant mode for electron production in the detection of such energetic radiations, each associated full energy peak is accompanied by two lower energy peaks corresponding to the escape of one or both of the 0.51-Mev annihilation quanta. Additionally, the relative intensity of these peaks is a function of crystal size and detection geometry. The low yield of full-energy contribution from high-energy radiation obtained with the small crystals used in the LRL installation produced a negligible sum-coincidence counting rate with the sum-discriminator window set at the binding energy. The solution is obvious: When looking for energy levels below ≈ 3 Mev (or >5 Mev for nuclei with added-neutron binding energy ≈ 8 Mev), the sum-discriminator window must be set 0.51 Mev down from the added-neutron binding energy so as to trigger on sums formed with the much more intense 1-escape annihilation peak of the high-energy radiation. When looking for energy levels between ≈ 3 and ≈ 5 Mev, the sum-discriminator window must be set 1.02 Mev down from the added-neutron binding energy so as to trigger on sums formed with the much more intense 1-escape annihilation peak from each of the high-energy radiations of the double cascade.

CONTAMINANTS

A cylinder of vanadium metal (naturally occurring, hence 0.24% V^{50} and 99.76% V^{51}) of diam $\frac{1}{4}$ in. and length $\frac{3}{4}$ in. was used for a target. The sample was cut from the center of a vanadium billet to avoid surface contaminations from a copper electrode used to prepare the solid metal. A chemical analysis revealed only negligible amounts of Si, Ca, Fe, and Cu. As a further test for purity, a small amount of the metal was irradiated in a 10^{13} neutron flux and the residual gamma radiation was analyzed. Radiation following beta decay was observed for Cu^{64} , Mn^{56} , and V^{52} showing that the sample contained a small amount of Mn in addition to the chemically determined contaminants. For the capture-gamma experiments the

target was suspended in a 10^5 thermal neutron beam at the end of a thin tube of plastic. Thus, other than negligible spectrum contamination from hydrogen and Al^{27} capture gammas (aluminum is used in the beam collimator), the radiations found should be principally from V^{52*} .

EXPERIMENTAL RESULTS

The capture-gamma singles spectrum in Fig. 3(a) clearly shows responses at 0.13, 0.42, 0.82, and 1.77 Mev (a possible Al^{28} beta-decay radiation contaminant) corresponding to ground-state transitions from (d,p)-determined V^{52*} levels.⁵ Notice that the 0.82-Mev indication is quite broad and thus may contain multiple radiations (e.g., 0.78 and 0.83 Mev). An intense V^{52} beta-decay radiation occurs at 1.43 Mev (verified by checking half-life with beam "off" after a prior irradiation) thus hiding ground-state transitions from possible 1.40, 1.48, and 1.55 Mev levels. Additionally, the strong Compton tail and lower energy plateau beginning at 1.25 Mev (which originates from the intense 1.43-Mev radiation) successfully masks any V^{52*} interlevel radiations which might have energies within this region. The strong 0.51-Mev peak is probably due to pair production in the target, shielding, or NaI crystals by high-energy V^{52*} radiation as well as by high-energy

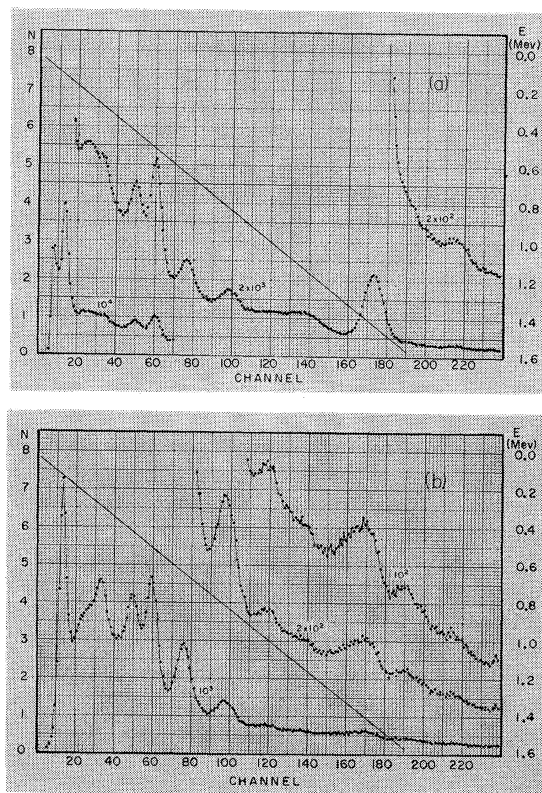


FIG. 3. (a) V^{52*} low-energy singles spectrum. The number beside the plot is counts per unit of N scale. (b) V^{52*} low-energy spectrum in total fast coincidence.

core gammas streaming down the neutron collimator and striking the target. Compton 180° backscattering may cause the buildup at 0.23 Mev, and the peak at 0.085 Mev has the right energy for Pb fluorescent radiation. The remaining strong peak at 0.65 Mev and the weak responses at 0.29, 0.34, 1.58, and 1.64 Mev are tentatively assigned to V^{52*} interlevel transitions.

In Fig. 3(b) a total fast-coincidence requirement (i.e., gating the analyzer to record only those quanta that are in fast coincidence with any other radiation in the spectrum) removes the 0.085-Mev Pb fluorescent radiation and the 1.43-Mev V^{52} beta-decay response. Now it is possible to see gamma evidence for transitions from 1.40- and 1.55-Mev levels to the ground state as well as additional buildups at 0.97 Mev (a possible Al^{28*} radiation), 1.00, 1.15, and 1.95 Mev (possible interlevel radiation). Also the 0.23-Mev Compton 180° backscattered peak is strongly degraded whereas a strong peak is now formed at the 0.29-Mev region. An additional total fast-coincidence experiment was made with scintillators oriented at 90° to each other for which the 0.23-Mev response disappeared and the 0.51-Mev peak was degraded thus showing that these radiations are not related to V^{52*} cascades.

Energy-discriminated fast-coincidence experiments

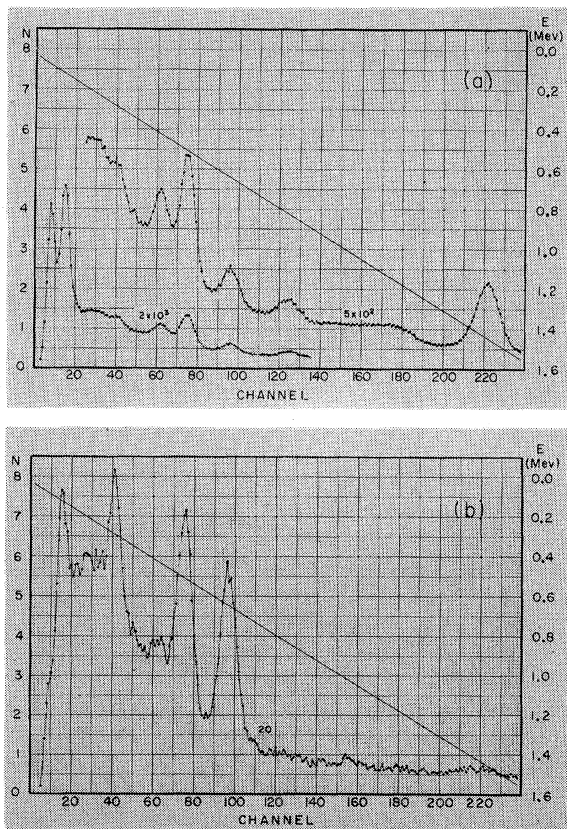


FIG. 4. (a) V^{52*} low-energy singles spectrum. The number beside the plot is counts per unit of N scale. (b) V^{52*} low-energy spectrum in fast coincidence with 0.130 Mev.

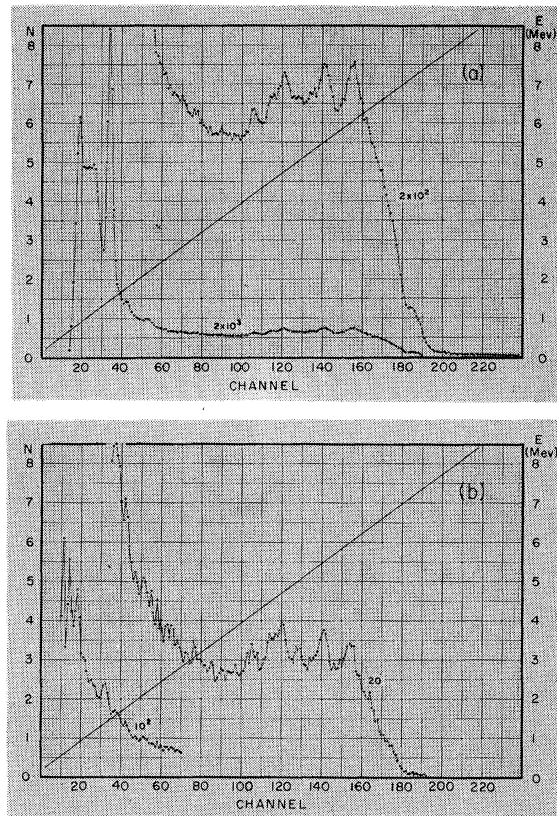


FIG. 5. (a) V^{52*} total singles spectrum. The number beside the plot is counts per unit of N scale. (b) V^{52*} total spectrum in fast coincidence with 0.51 Mev.

were made in the low-energy spectrum to explore the decay scheme. As a shorthand notation for the following cascade discussions, a transition from level A to level B with the release of radiation having energy $(A-B)$ Mev will be written as $A(A-B)B$. Triggering on 0.13 Mev, Fig. 4(b), strong coincidences were found with 0.29, 0.51, and 0.65-Mev radiations and a weaker 1.96 response (not shown), thus suggesting 0.42(0.29)0.13, 0.78(0.65)0.13, and 2.09(1.96)0.13 Mev transitions. The strong 0.51 peak in the coincidence spectrum can be expected from pair production by high-energy gammas in coincidence with 0.13. Only a very weak indication of coincidence with 0.70 was observed for a possible 0.83(0.70)0.13 Mev de-excitation. Other very weak responses (such as at 0.20, 0.34, and 1.01 Mev) were observed for possible coincidences with 0.13; however, these indications were not accepted as significant because they are not strong enough to be clearly outside of statistical fluctuations. The $0.42 \times (0.29)0.13$ and $0.78(0.65)0.13$ cascades were checked by triggering on 0.29 and 0.65 Mev separately, for which only strong 0.13 and 0.51-Mev coincidences were obtained. A weak (but sufficient) 0.13-Mev response was received for triggering on 1.96 Mev to establish a low-intensity 2.09(1.96)0.13 transition.

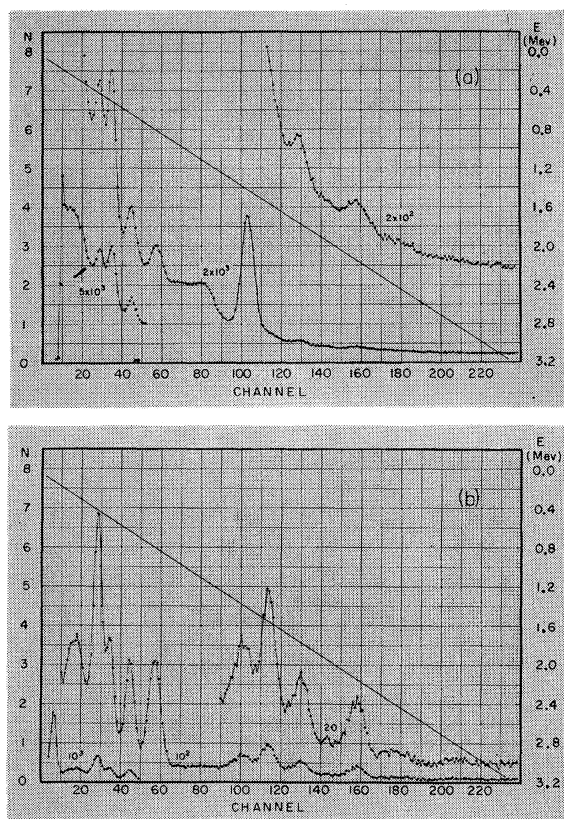


FIG. 6. (a) V^{52*} low-energy singles spectrum. The number beside the plot is counts per unit of N scale. (b) V^{52*} low-energy sum-coincidence spectrum (sum = $7.31 - 0.51 = 6.80$ Mev).

Setting the discriminator on 0.42 Mev, weak coincidences were observed with 0.98, 1.06, and a broad 1.40 Mev but there was no evidence for a 0.78(0.36)0.42 cascade. Other coincidence experiments suggested very weak 1.84(0.44)1.40, 1.84(1.06)0.78, 1.79(1.37)0.42, 1.48(1.06)0.42, 1.48(0.70)0.78, 1.40(0.98)0.42, and 1.40 \times (0.62)0.78 transitions, but these cascades were too doubtful to be assigned. Energy resolution was not adequate to probe with a narrow discriminator window for a 0.83(0.41)0.42 de-excitation. A broad window covering 0.39 to 0.44 Mev, however, did not indicate coincidence between 0.41 and 0.42 Mev and consequently this cascade must be very weak if it exists at all.

Figure 5(a) presents the total singles-radiation spectrum which is difficult to interpret because of multiple (i.e., escape) peaks inherent in high-energy scintillation spectroscopy. The full energy peak for the 7.31-Mev ground-state transition is barely discernible; however, the full energy peak for a 7.18-Mev transition to the 0.13 level is very apparent. Strong peaks occur at 6.0 and 5.5 Mev which appear to be 1- and 2-escape peaks (the full energy peak is obscure) for 6.5-Mev transitions to the 0.78- and 0.83-Mev levels. Similarly the peaks at 4.75 and 4.2 Mev must be 1- and 2-escape

peaks for 5.2-Mev radiation to the multiple levels in the 2.1 region, and the much weaker indications at 5.0 and 4.5 Mev are probably 1- and 2-escape peaks for 5.5-Mev de-excitations to the 1.8-Mev multiple level region. Here the 5.2-Mev radiation appears markedly more intense than the 5.5-Mev radiation, whereas Groshev *et al.*⁷⁻⁹ measured absolute intensities of 6.5 and 7.2 photons/100 captures, respectively. Figure 5(b) shows an improvement for the high-energy spectrum, obtained by converting the coincidence spectrometer into a 2-crystal pair spectrometer (i.e., triggering on 0.51 radiation in the conventional coincidence mode) thus eliminating full energy peaks. Only 1- and 2-escape peaks appear in the upper spectrum of Fig. 5(b) and it is now possible (but not profitable) to analyze this portion of the display. Both Bartholomew and Kinsey and Groshev *et al.* have thoroughly explored the V^{52*} high-energy radiations with vastly more suitable equipment and have reported very similar findings. Upper spectrum displays are presented here merely as a matter of interest and to demonstrate the experimental problem. The lower spectrum of Fig. 5(b), however, is profitable to examine and shows V^{52*} radiations at 1.00, 1.10, 1.40, 1.55, 1.78, 1.96, 2.10, 2.35, 2.42, 2.53, 2.65, 3.05, 3.19, 3.40 Mev, and higher energies.

Although the scintillation coincidence spectrometer is not intended for high-energy work, it is very suitable for checking the neutron binding energy in nuclei by electronically summing the output of the two detectors and then observing the sum spectrum (i.e., the output of the adding network) with a fast-coincidence requirement. The asymptotic intersect of the high-energy sum response with the base line indicated a binding energy of 7.30 ± 0.05 Mev for the added neutron in V^{52} , which agrees with the values of 7.305 ± 0.007 and 7.30 ± 0.015 Mev obtained by Bartholomew and Kinsey and Groshev *et al.*, respectively. Additionally, the low-energy portion of the sum spectrum showed a prominent peak at 0.78 Mev and only the suggestion of a buildup at 0.83 Mev. This evidence indicates that very few if any 0.83(0.41)0.42 or 0.83(0.70)0.13 transitions occur.

A particularly helpful experiment was made with the Hoogenboom sumcoincidence technique for observing double cascades.¹² Unfortunately the counting rate was impractically low with the sum discriminator set at the binding energy, and it was necessary to set the discriminator 0.51 Mev below the binding energy (i.e., $7.31 - 0.51 = 6.80$ Mev) for triggering from the more intense 1-escape peak. A reasonable counting rate was then obtained with a 0.25-Mev-wide discriminator window which, after three days running time, produced the results shown in Fig. 6(b). In order to interpret this spectrum it must be realized that the 0.25-Mev-wide discriminator window permits sums with transitions from excited levels to the 0.13 Mev level as well as to the ground state. Notice in particular how level structure in the 1.4-Mev region now becomes evident

whereas this region is saturated in the singles spectrum by the 1.43-Mev V^{52} beta-decay radiation. A detailed study of the sum-coincidence spectrum and associated data reveals the radiations listed in Table I and the decay scheme (which was matched to fit the level scheme suggested in reference 5) presented in Fig. 7.

DISCUSSION

El Bedewi and Tadros¹⁰ have recently studied angular distributions for the $V^{51}(d,p)V^{52*}$ reaction and report that the 29th neutron carries one unit of orbital angular momentum into the ground state and consequently is captured in the $2p_{3/2}$ state. This important work shows that, at least in V^{52} , the $2p_{3/2}$ state occurs at a lesser energy than the $1f_{5/2}$ state.

TABLE I. Low-energy V^{52} capture gamma rays. Energies in Mev.

Schwäger	Groshev <i>et al.</i> (reference 7)	Reier and Shamos ^c
3.40±0.03
(3.19±0.04) ^a
3.05±0.03
(3.00±0.04)
2.85±0.03	2.85±0.02	...
(2.73±0.04)
2.65±0.03
2.53±0.03
2.48±0.03
...	2.44±0.02	...
(2.42±0.04)
(2.36±0.04)
2.32±0.03	2.30±0.02	...
...	...	2.25±0.03
(2.19±0.03)
2.15±0.02
...	2.13±0.01	...
(2.12±0.03)
(2.08±0.03)
(2.00±0.03)	2.02±0.02	...
1.95±0.02	1.93±0.015	...
(1.85±0.03)
1.78±0.02	1.77±0.01	...
(1.73±0.03)
1.70±0.02
(1.67±0.03)
...	1.65±0.01	...
(1.63±0.03)
1.56±0.02	1.55±0.01	...
1.48±0.02
1.43±0.02 ^b	1.434±0.005 ^b	1.46±0.03 ^b
1.42±0.02
1.38±0.02
1.15±0.02
1.10±0.02
(1.06±0.02)
1.00±0.02
(0.83±0.02)	0.84±0.01	0.84±0.03
(0.78±0.02)	0.79±0.015	...
(0.70±0.02)
0.64±0.02	0.652±0.005	0.63±0.03
(0.62±0.02)
(0.44±0.02)
0.42±0.02	0.42±0.01	0.42±0.03
0.34±0.02
0.29±0.01
0.13±0.01

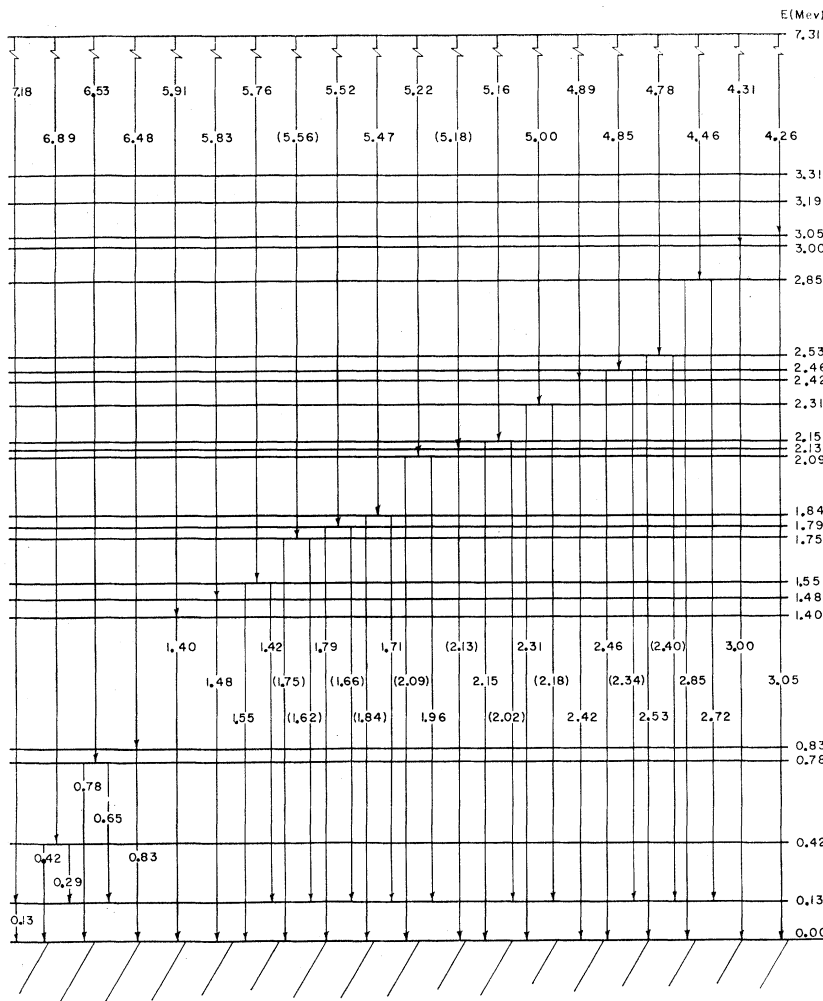
^a Parentheses indicate weak or unresolved response.^b Gamma ray following beta decay of V^{52} .^c M. Reier and M. H. Shamos, Phys. Rev. **95**, 636 (1954).

The shell model assures us that V^{52} must have an even-parity ground state, but the spin (not yet measured) is ambiguous because reliable coupling rules have not yet been established for odd-odd nuclei. However, V^{52} is unstable and beta decays¹⁴ with $\log ft=5.5$ to the Cr^{52*} 1.43-Mev level (even-even nucleus, hence even spin and parity). This is an allowed transition and, according to Gamow-Teller selection rules, the spin change can be 0 or ± 1 for the decay. Since El Bedewi and Tadros¹⁵ report 2^+ spin for the Cr^{52*} 1.43 level, the V^{52} ground state might have 1^+ , 2^+ , or 3^+ spin, all of which are possible for coupling between a $(1f_{7/2})^3$ proton configuration and a $2p_{3/2}$ neutron. A spin of 1^+ is improbable, however, because otherwise V^{52} should decay to the Cr^{52} 0^+ spin ground state. Also, the V^{52*} capture state must be 3^- or 4^- spin and the reported 7.31-Mev ground-state transition seems too intense for $M2$ or $E3$ radiation. Thus a ground spin of 2^+ or 3^+ is expected for V^{52} and, when established, will be a test of Nordheim's rule which indicates the spin should be 3^+ .

All of the low-lying V^{52*} levels are expected to have even parity. It was not possible in the present work to suggest spins for any of these levels; however, some of the experimental findings may help later to make spin assignments. Since the fast-coincidence unit has a time resolution of 4×10^{-8} second, the 0.13-Mev radiation observed in the coincidence spectrum may be an $M1$ transition although one hastens to add that $E2$ transitions are known to occur often with comparable transition time. Several crossover, without stopover, transitions are observed: two from the 0.78-Mev level to the ground and 0.13-Mev levels (the latter being the more intense) but not to the 0.42-Mev level, and one from the 0.83-Mev level to the ground state only. On the other hand, the 0.42-Mev level makes both crossover and stopover transitions to the ground and 0.13-Mev levels (the former being the stronger).

Coupling between a $(1f_{7/2})^3$ proton configuration and a $2p_{3/2}$ neutron produces 2 states with spin 0^+ , 1 of 1^+ , 3 of 2^+ , 3 of 3^+ , 5 of 4^+ , 3 of 5^+ , 3 of 6^+ , 2 of 7^+ , 1 of 8^+ , and 1 of 9^+ for a total of 24 possible states. One might argue that it is reasonable to expect the interaction energy to be small between particles that differ considerably in radial and azimuthal quantum numbers (i.e., $1f_{7/2}$ vs $2p_{3/2}$) compared with the interaction of particles in the same orbit (otherwise the shell model would not be a good approximation), and thus the low excited states could arise from excitation of the $(1f_{7/2})^3$ proton configuration alone. There is weak evidence to infer that this situation occurs. First, El Bedewi and Tadros¹⁰ found from $V^{51}(d,p)V^{52*}$ proton distributions that the 29th neutron appears to have orbital angular

¹⁴ Nuclear Shell Schemes, compiled by R. N. King, C. L. McGinnis, and R. van Lieshout, Atomic Energy Commission Report TID-5300 (U. S. Government Printing Office, Washington D. C., 1955).¹⁵ F. A. El Bedewi and S. Tadros, Nuclear Phys. **6**, 434 (1958).

FIG. 7. Gamma-ray decay in V^{52} .

momentum of unity in the ground and first eight levels. Second, there is surprising consistency in the relative level spacing between the four lowest excited states of V^{51*} and V^{52*} (the author shows in another paper that the ground and four lowest levels in V^{51*} belong to the $(1f_{7/2})^3$ configuration), which might represent similar states that have been depressed by the additional (i.e., 29th) neutron. Third, all but one of these levels (0.42 Mev) show large (d,p) capture probability^{5,10} which suggests that these levels have proton configurations the same as in V^{51} .

Additional work, such as gamma-gamma angular correlations, is needed to clarify the data.

ACKNOWLEDGMENTS

I wish to thank Professor Burton J. Moyer for his guidance during the course of this work. The help of Dr. Laurence Passell and Dr. Harry West during the initial development of the spectrometer is profoundly appreciated. Transcending these acknowledgements, I am indebted to Dr. Edward Teller, Dr. Herbert York, Dr. Albert Kirschbaum, and Dr. James Carothers for encouraging and generously supporting the experimental program, and to Vice Admiral John T. Hayward, U. S. Navy, Rear Admiral Frederick L. Ashworth, U. S. Navy, and Professor Leonard B. Leob who have motivated my interest in science.

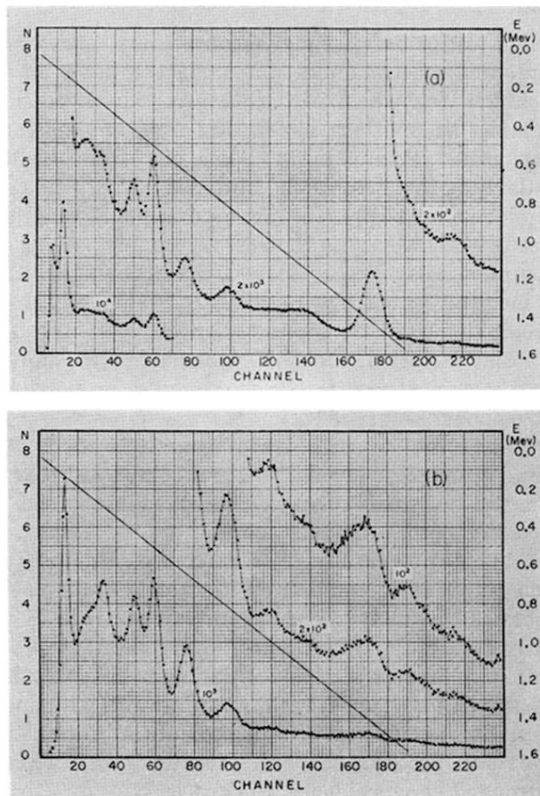


FIG. 3. (a) V^{52*} low-energy singles spectrum. The number beside the plot is counts per unit of N scale. (b) V^{52*} low-energy spectrum in total fast coincidence.

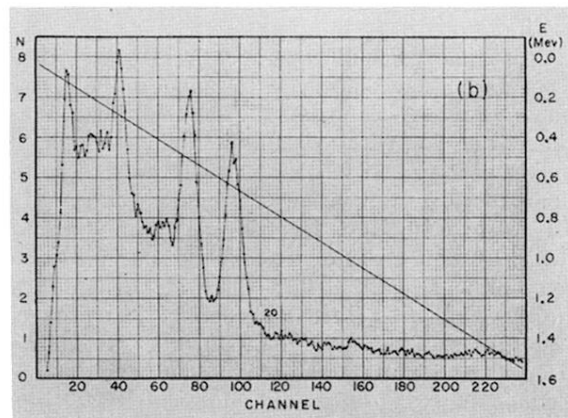
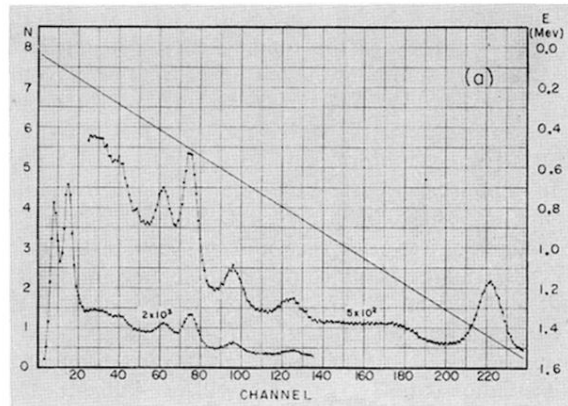


FIG. 4. (a) V^{52*} low-energy singles spectrum. The number beside the plot is counts per unit of N scale. (b) V^{52*} low-energy spectrum in fast coincidence with 0.130 Mev.

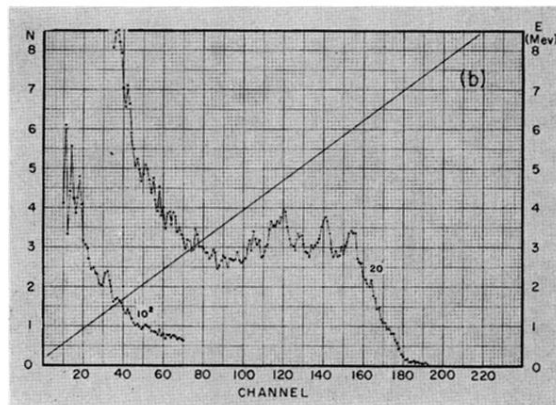
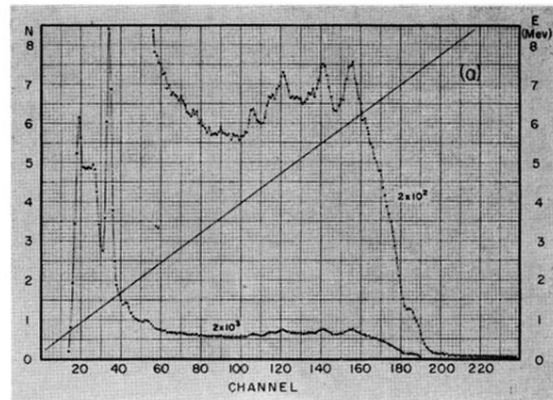


FIG. 5. (a) V^{52*} total singles spectrum. The number beside the plot is counts per unit of N scale. (b) V^{52*} total spectrum in fast coincidence with 0.51 Mev.

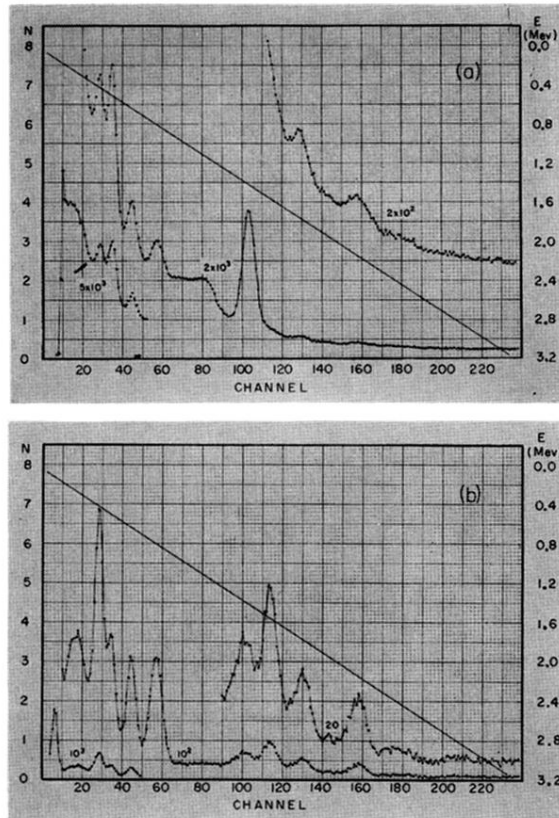


FIG. 6. (a) V^{52*} low-energy singles spectrum. The number beside the plot is counts per unit of N scale. (b) V^{52*} low-energy sum-coincidence spectrum ($\text{sum} = 7.31 - 0.51 = 6.80$ Mev).